

N 9 4 - 2 3 0 3 5

**EVAPORATION AND COMBUSTION OF LOX UNDER SUPERCRITICAL AND SUBCRITICAL CONDITIONS\***

A. S. Yang, ‡ W. H. Hsieh, † and K. K. Kuo §

Propulsion Engineering Research Center  
and

Department of Mechanical Engineering  
The Pennsylvania State University  
University Park, PA 16802

**SUMMARY:**

The objective of this investigation is to study the evaporation and combustion of LOX under supercritical and subcritical conditions both experimentally and theoretically. In the evaporation studies, evaporation rate and surface temperature were measured when LOX vaporizing in helium environments at pressures ranging from 5 to 68 atm. A Varian 3700 gas chromatograph was employed to measure the oxygen concentration above the LOX surface. For the combustion tests, high-magnification video photography was used to record direct images of the flame shape of a LOX/H<sub>2</sub>/He laminar diffusion flame. The gas composition in the post-flame region is also being measured with the gas sampling and chromatography analysis. These data are being used to validate the theoretical model. A comprehensive theoretical model with the consideration of the solubility of ambient gases as well as variable thermophysical properties was formulated and solved numerically to study the gasification and burning of LOX at elevated pressures. The calculated flame shape agreed reasonably well with the edge of the observed luminous flame surface. The effect of gravity on the flame structure of laminar diffusion flames was found to be significant. In addition, the predicted results using the flame-sheet model were compared with those based upon full equilibrium calculations (which considered the formation of intermediate species) at supercritical pressures. Except at the flame front where temperature exceeded 2,800 K, the flame-sheet and equilibrium solutions in terms of temperature distributions were in very close agreement. The temperature deviation in the neighborhood of the flame front is caused by the effect of high-temperature dissociation.

**TECHNICAL DISCUSSION:**

Liquid oxygen (LOX) and hydrogen have been used in various types of liquid rocket engines because of their high specific impulse and low exhaust pollution.[1] Inside a liquid rocket engine, the oxygen and hydrogen are injected into a combustion chamber. Through the large shear force between the fuel and oxidizer streams, the primary atomization of oxygen is accomplished to form a spray of droplets. The vaporizing behavior of a single LOX droplet in high-pressure

\* This paper represents a part of the research work sponsored by NASA/MSFC and PSU/PERC. The encouragement and support of Mr. Klaus Gross of MSFC are highly appreciated.

‡ Ph.D. Candidate

† Assistant Professor

§ Distinguished Professor and Director of the High Pressure Combustion Lab

hydrogen-rich environments has been studied extensively by Litchford and Jeng[2], Delplanque and Sirignano[3], and Yang et al.[4] However, no comparison of their predictions with experimental data was established for these evaporation studies due to the unavailability of testing results.

One of the major obstacles involved in the evaporation and combustion studies of a single droplet is that the size of a typical LOX droplet is usually too small to allow detailed measurements of flow properties in its neighborhood. In order to overcome this problem, a liquid strand test setup has been employed to maintain the surface of the liquid oxygen at a fixed location. In the LOX feeding system, gaseous oxygen was delivered into a cylinder immersed in a liquid nitrogen bath. Cooled by liquid  $N_2$ , the oxygen was liquefied and eventually filled in the interior space of a cylinder serving as a reservoir for LOX. By adjusting the opening of a micro-metering valve, the LOX mass consumption rate can be satisfactorily controlled to maintain a stable surface at the exit of the LOX feeding tube under prespecified steady-state operating conditions. In combustion tests, ignition of LOX with the surrounding hydrogen was achieved using a spiral nichrome-wire ignitor. The chamber pressure was maintained at a prespecified level by a computer feedback-controlled gas purging system. The surface temperature at the exit of the LOX feeding tube was measured using a  $75\ \mu\text{m}$  Fe/Cu-Ni (J-type) fine-wire thermocouple. Direct images of the flame shape of a LOX/hydrogen laminar diffusion flame were also recorded using high-magnification video photography. For species concentration measurements, a quartz micro-probe with an orifice diameter of  $25\ \mu\text{m}$  is used to sample the gas mixture in the post-flame region. The gas mixture composition is measured using a Varian 3700 gas chromatograph (GC) with a thermal conductivity detector. Detailed description of the experimental setup can be found in Ref. 5.

Theoretically, a comprehensive model was formulated to simulate the evaporation and combustion processes of liquid oxygen with the hydrogen/helium mixture at elevated pressures. The model was based on the conservation equations of mass, momentum, energy, and species concentrations for a multi-component system. With allowance for the axial diffusion, the model described by a set of coupled elliptic partial differential equations was solved numerically. The gravitational body force was considered to account for the influence of natural convection. In the treatment of the real-gas behavior, pressure and temperature effects were included for evaluating thermodynamic and transport properties.[5] The flame-sheet approximation with consideration different mass diffusivities for individual species was used to model the combustion process of oxygen and hydrogen under supercritical conditions. To characterize the high-pressure solubility of the ambient gas into the liquid, a fugacity-based multicomponent thermodynamic analysis with quantum-gas mixing rules was also carried out. Calculations were performed by solving the governing equations with an iterative SIMPLE (Semi-Implicit Method for Pressure-Linked Equations) algorithm.

Results obtained in the evaporation study are given in Ref. 6. Results from the combustion study are presented and discussed as follows. In the combustion tests, a stable onion-shaped LOX/ $H_2$ /He diffusion flame was achieved at a pressure of 30 atm. (The laminar diffusion flame studied had a oxygen supply rate of 0.018 gm/s, hydrogen of 0.052 gm/s, and helium of 0.12 gm/s.) However, the LOX surface was below the exit of the feeding tube by about 1.5 mm. To raise the

LOX surface to the port of the feeding tube, the oxygen supply rate was gradually increased to 0.024 gm/s. When the LOX surface approached to the tube exit, the region near the tube rim was cooled down significantly by the LOX. This decrease in temperature caused the increase of heat loss from the flame as well as reducing radical concentrations in chemical reactions. Thus, the flame tended to detach from the tube rim and became unstable. This quenching effect sometimes even caused extinguishment of the flame.

To verify the present axisymmetric steady-state combustion code, a numerical simulation was conducted by considering the LOX surface fixed at the position of 1.5 mm below the exit of the feeding tube. From surface temperature measurements, the LOX surface was 136.2 K at  $P = 30$  atm. The temperature of the surrounding hydrogen/helium mixture was 295 K. Based on measured mass flow rates of oxygen, hydrogen, and helium, the gas velocities of the H<sub>2</sub>/He mixture flow and vaporized LOX were 1.5 and 0.523 cm/s, respectively. The oxygen mass fraction at the LOX surface was also determined to be 0.981 from the phase equilibrium analysis. Figure 1 presents the comparison between predicted and experimentally-observed steady flame shape for the coflowing LOX/H<sub>2</sub>/He laminar diffusion flame at a pressure of 30 atm. In general, the calculated flame shape was in reasonable agreement with the observed luminous flame surface. In the prediction of the flame height, the calculated flame front was found to be very close to the edge of observed flame surface (as shown in Fig. 2). More measurements of the species concentration in the post-flame region are being conducted with a gas sampling system coupled with a GC for further code validation.

To study the influence of the LOX surface position on the flame shape, another simulation was conducted for the case in which the LOX surface was maintained at the exit of the feeding tube. Same boundary conditions (as used in the former case study) were employed except that the oxygen supply rate was increased from 0.018 to 0.024 gm/s. Corresponding to this flow rate, the gas velocity above the LOX surface was 0.7 cm/s. Figure 3 presents the predicted and observed flame shape at a pressure of 30 atm. In a global view, the size of the calculated flame zone becomes larger when the LOX surface moves to the exit plane of the port. Compared to the former case, the flame height (defined by the axial distance between the locations of the LOX surface and the peak temperature) increased from 7.1 to 12.0 mm.

The theoretical model was also used to predict the structure of a LOX/H<sub>2</sub>/He laminar diffusion flame with a H<sub>2</sub>/He mass ratio of 30/70 at a pressure of 68 atmospheres. The inflow velocity of vaporized oxygen was 0.218 cm/s above the LOX surface and the flow velocity of the surrounding hydrogen/helium mixture was 1.5 cm/s. The temperatures of the LOX surface and the surrounding flow were 153.3 and 295 K, respectively. The phase equilibrium analysis was applied to determine boundary conditions of species concentration at the LOX surface. The oxygen mass fraction at the LOX surface was 0.988 in this case.

Figure 4 shows temperature contours with respect to both axial and radial coordinates. In general, the high temperature area spanned from the interface region of the oxidizer and fuel inlets near the tube rim to the center line. The peak temperature along the center line was about 3310

K. The flame height was found to be 1.66 cm above the tube exit. The steep axial temperature gradients were noted in the vicinity of the LOX surface, which indicated a strong heat feedback from the flame to the LOX surface, to provide the energy required in the phase change of oxygen from a compressed liquid to a superheated vapor. To examine the effect of gravity on the flame structure, another calculation (using same boundary conditions) was performed with zero gravity. Figure 5 exhibits temperature contours without considering the body-force effect. Compared with Fig. 4, significant difference in the temperature plot is noted as the gravity term is removed from the axial momentum equation. In the case with gravity effect, the buoyancy force accelerates the flow in the reaction zone and thereby increases the entrainment of the surrounding  $H_2/He$  mixture. This suction-like effect induces an inward radial flow motion near the port exit plane to enhance combustion and drive the flame closer to the center line. In contrast to the above case, the flame tends to expand in the radial direction and its flame height is taller at the zero-gravity condition. This result demonstrates that the buoyancy effect can be very important in influencing the shape of diffusion flame. These results can be utilized to interpret flame structures under microgravity conditions.

To examine the reaction zone broadening due to dissociation, the predicted temperature distribution along the centerline from the flame-sheet model is compared with that of equilibrium calculations, which considered the formation of intermediate species such as hydrogen atom, oxygen atom and hydroxyl radical in the flame. Figure 6 presents the comparison of these two solutions. Below 2,800 K, the difference was found to be within 2.5%. However, the flame-sheet model with no dissociation overpredicted the peak temperature by 8.5% at the axial location of the flame front ( $x = 1.66$  cm). This discrepancy is obviously attributed to the fact that intermediate species produced in the dissociation process are considered in the equilibrium solution.

#### REFERENCES:

1. Sutton, G. P., *Rocket Propulsion Elements*, John Wiley & Sons, New York, 1986.
2. Litchford, R. J. and Jeng, S. M., "LOX Vaporization in High-Pressure, Hydrogen-Rich Gas," AIAA Paper No. 90-2191, 1990.
3. Delplanque, J. P. and Sirignano, W. A., "Transient Vaporization and Burning for an Oxygen Droplet at Sub- and Near-Critical Conditions," AIAA Paper No. 91-75, 1991.
4. Yang, V., Lin, N. N., and Shuen, J. S., "Vaporization of Liquid Oxygen (LOX) Droplets at Supercritical Conditions," AIAA Paper No. 92-103, 1992.
5. Kuo, K. K., Hsieh, W. H., Yang, A. S., and Brown, J. J., "Combustion of LOX with  $H_{2(g)}$  under Subcritical, Critical, and Supercritical Conditions," Annual Report to NASA/MSFC, February, 1992.
6. Yang, A. S., Hsieh, W. H., Kuo, K. K., and Brown, J. J., "Evaporation of LOX under Supercritical and Subcritical Conditions," AIAA Paper No. 93-2188, 1993.

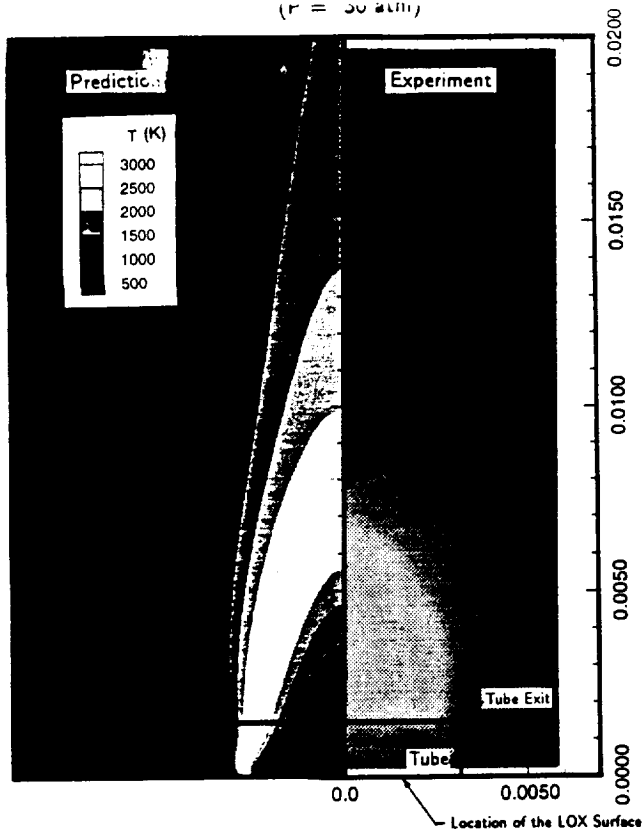


Figure 1 Predicted and Experimentally-observed Flame Shape with an Oxygen Supply Rate of 0.018 gm/sec at a Pressure of 30 atm

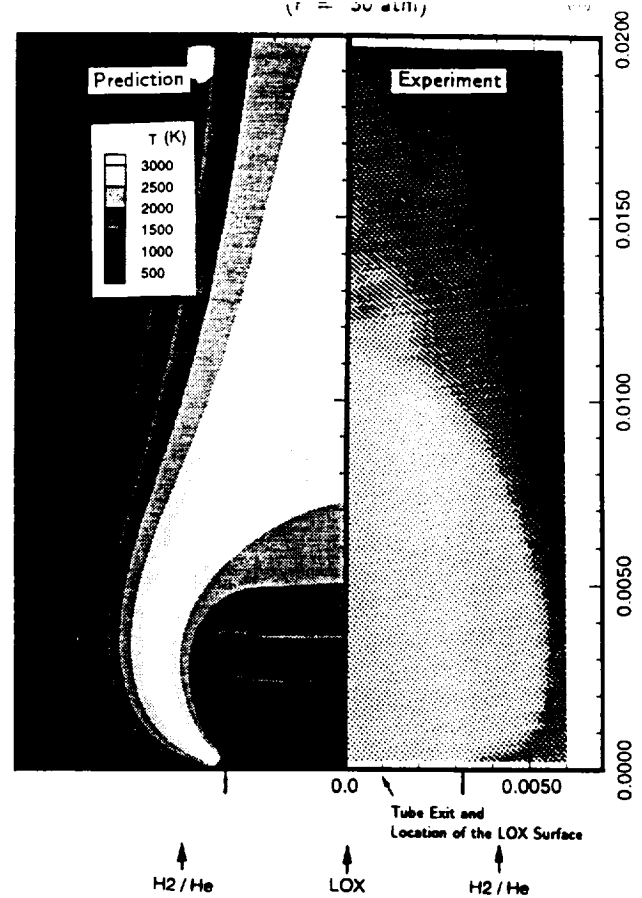


Figure 3 Predicted and Experimentally-observed Flame Shape with an Oxygen Supply Rate of 0.024 gm/sec at a Pressure of 30 atm

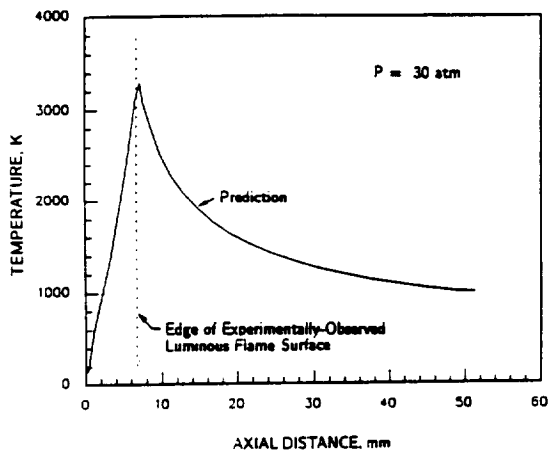


Figure 2 Predicted Center-line Temperature Profile and Location of Luminous Flame Surface at a Pressure of 30 atm

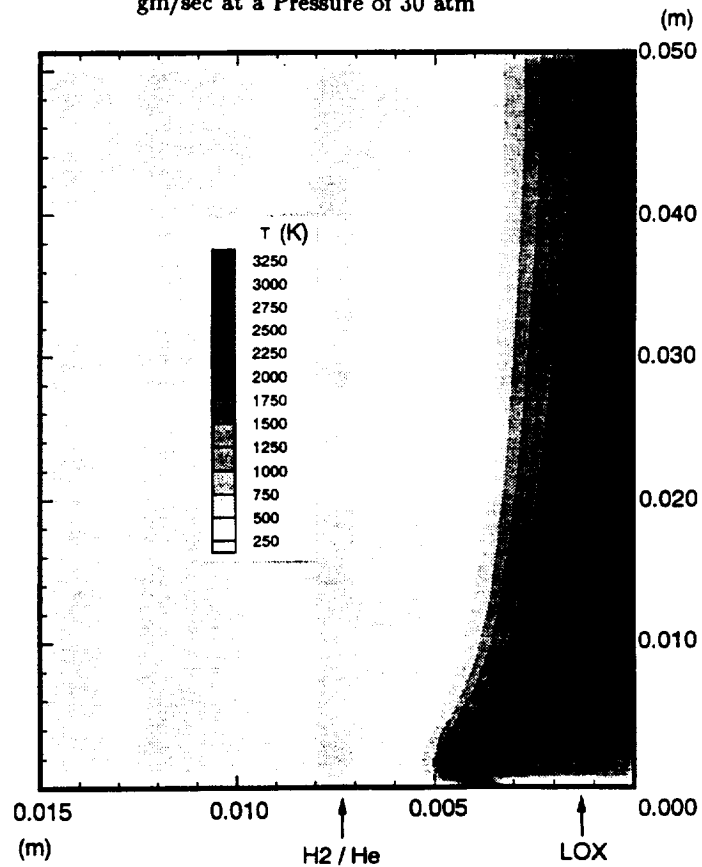


Figure 4 Temperature Contour for the Coflowing LOX/Hydrogen/Helium Laminar Diffusion Flame at a Pressure of 68 atm

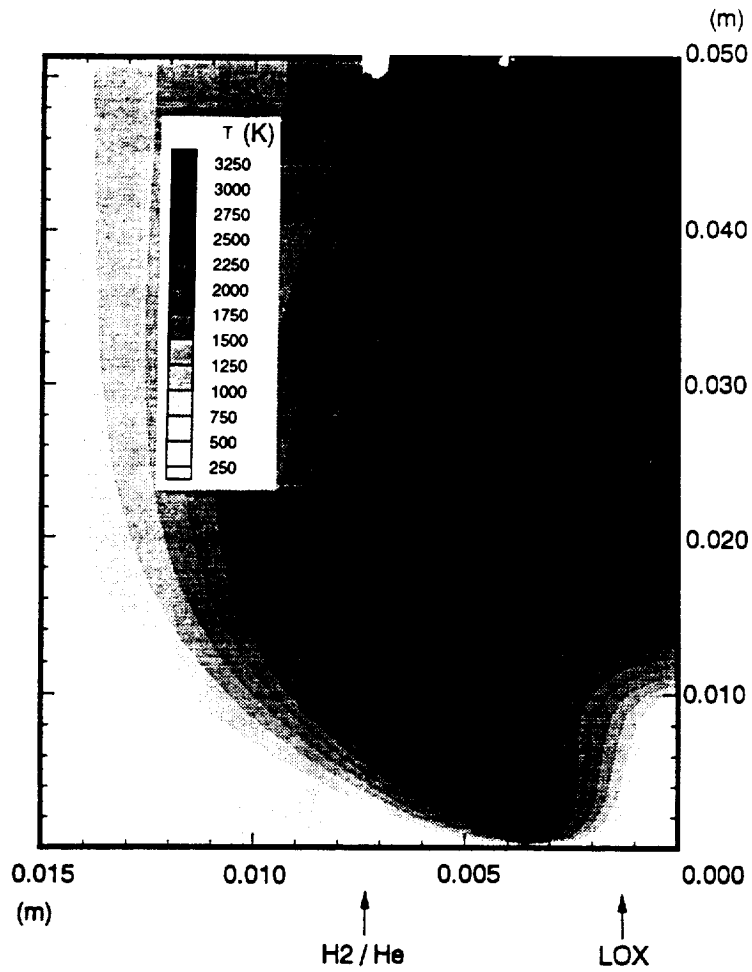


Figure 5 Temperature Contour for the Coflowing LOX/  
Hydrogen/Helium Laminar Diffusion Flame with-  
out the Effect of Gravity ( $P = 68$  atm)

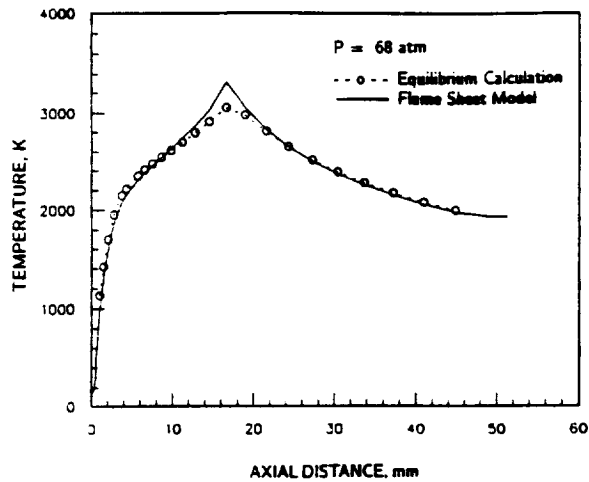


Figure 6 Comparison between Equilibrium Calculations  
and the Predicted Center-line Temperature Pro-  
file ( $P = 68$  atm)